Temperature sensor based on luminescence intensity ratio or whispering gallery modes in phosphate glass co-doped with Pr^{3+} and Yb^{3+}

H. Benrejeb[a,b], IR. Martin[c,d], S. Hraiech[b], K. Soler-Carracedo[c]

[a] Université de Carthage, Faculté des sciences de Bizerte, 7021, Zarzouna Bizerte, Tunisie.

[b] Physical Chemistry Laboratory of Mineral Materials and their Applications, National Center of Research in Materials Sciences, B.P. 73, 8027 Soliman, Tunisia.

[c] Departamento de Física, Universidad de La Laguna. Apdo. 456. E-38200 San Cristóbal de La Laguna, Santa Cruz de Tenerife, Spain.

[d] Instituto Universitario de Materiales y Nanotecnología (IMN), Universidad de La Laguna. Apdo. 456. E-38200 San Cristóbal de La Laguna, Santa Cruz de Tenerife, Spain.

Abstract

Microspheres of diameters ranging from 30 μm to 100 μm, obtained from $0.1Pr^{3+}$-$0.5Yb^{3+}$ co-doped phosphate glass were fabricated and calibrated as optical temperature sensor. When the microspheres where pumped under 457 nm laser excitation, Pr^{3+} typical emission was observed as well as emission due to a Down Conversion (DC) process from Pr^{3+} to Yb^{3+} ions. Furthermore, whispering gallery modes (WGM) peaks superimposed to the Pr^{3+} and DC emission bands were observed. The microsphere was calibrated as a function of temperature using the intensity ratio of the 925 and 875 nm Pr^{3+} bands and the spectral red-shift from the WGM. Temperature uncertainty was obtained from both techniques obtaining values of 0.7 K and 0.4 K for the band ratio and WGM results, respectively.

Keywords: biological window; optical sensor; lanthanide ions; microsphere resonators

1. Introduction

Temperature is a fundamental thermodynamic parameter, which has always been one of the most important parameters to consider in a wide variety of disciplines from science to industry, among others such as astrophysics, chemistry, biomedicine and biophysical [1–4]. All of this makes the need of new temperature sensors a highly demanded field that is in continuous development. In the last decades, a new sort of optical temperature sensor has received much more interest thanks to its several advantages such as better sensitivity, quick response, contactless method, high thermal resolution and good precision [5–8]. Due to their rich energy-level structure, Rare earth (RE) doped as dopants for different host matrix are pretty suitable for optical temperature sensors, using the luminescence intensity ratio (LIR) technique to monitor temperature. In this method, optical temperature measurement is based on the changing of the emission intensity ratio with the

temperature from two emitting levels [9–11]. As a particular case, if these excited emitting levels are thermally coupled, then there is a temperature dependent population redistribution that follows the Boltzman law and the technique is usually called fluorescence intensity ratio (FIR) technique. On the other hand, RE doped glasses can be used as an optical temperature sensor providing the optically active glass is shaped as a micro-resonator. The spectroscopic characteristic of the emission obtained from a luminescent micro-resonator is the appearance of very sharp modes of resonances in the emission spectra. In this context, a group of optical micro-systems called Whispering Gallery Modes (WGM) has attracted great research interest and studied as optical temperature sensors [12]. These sensors are based on the fact that any change in the temperature inside the micro-cavity leads to a shift in the wavelength of the resonances. One of the advantages of WGM is the quick time resolution, on the order of tens of milliseconds, in addition to their high response to any external fields as well as environment changes that influence the refractive index [13].

In order to explore a developing possibility of optical high temperature sensor based on the FIR technique and WGM, we have prepared for the first time microspheres from phosphate glass co-doped with $0.1Pr^{3+}$-$0.5Yb^{3+}$. Among the advantages of this sensor, it includes its relatively easy synthesis and great transparency from the ultraviolet (UV) to the mid infra-red (IR) region. The temperature response was obtained using the intensity ratio of the 925 and 875 nm Pr^{3+} bands (LIR) or the spectral red-shift from the WGM. The possibility of using these wavelengths, both located in the "first biological window" (I-BW) range, for contactless temperature calibration; represents another advantage of using Pr^{3+} over other RE candidates. The sensor shows uncertainty values of less than 1 K in the case of the LIR technique and less than 0.5 K for the WGM. These values obtained for phosphate glass microspheres co-doped with $0.1Pr^{3+}$-$0.5Yb^{3+}$ predicts this material as a promising candidate for temperature sensing.

Experimental

Phosphate glasses with compositions of $39.4P_2O_5$-$40Na_2O$-$18ZnO$-$2Al_2O_3$-$0.1Pr_2O_3$-$0.5Yb_2O_3$ were prepared by the conventional melting-quenching method. Reagent of $NH_4H_2PO_4$, Na_2CO_3, ZnO, Al_2O_3, Pr_2O_3 and Yb_2O_3 were used as raw materials. The chemical reagents were carefully mixed using a mortar, and melted at 900°C for 3h. The glasses obtained were annealed at 200°C for 12h and slowly cooled down to room temperature (RT).

The absorption spectrum of $0.1Pr^{3+}$-$0.5Yb^{3+}$ co-doped phosphate glass in the range from 400 to 2500 nm was measured with a double beam spectrophotometer (Cary Series UV-VIS-NIR Spectrophotometer from Agilent Technologies).

Using the glass mentioned above, microspheres were fabricated following the method exposed by Gregor R. Elliott et al. [14]. These include polishing, chemical etching and rapid quenching of liquid droplets [15]. As a result, microspheres of diameters ranging from 30 μm to 100 μm were obtained.

Spectral emission was obtained by exciting the material with a continuous-wave 457 nm diode pumped solid state laser. For excitation and detection, a modified confocal microscope was used, collecting the light emitted by the sample with an objective and then focused it on the entrance slit of a grating spectrometer (Andor SR-500i-B2), coupled to a CCD (Newton 970EMCCD) detector. An adjustable mirror, combined with the entrance slit (~60 μm) acting as an image plane pinhole, allowed to partially detect the emission from localized parts of the microsphere [16] (Fig. 1). All spectra were corrected from the spectral response of the equipment.

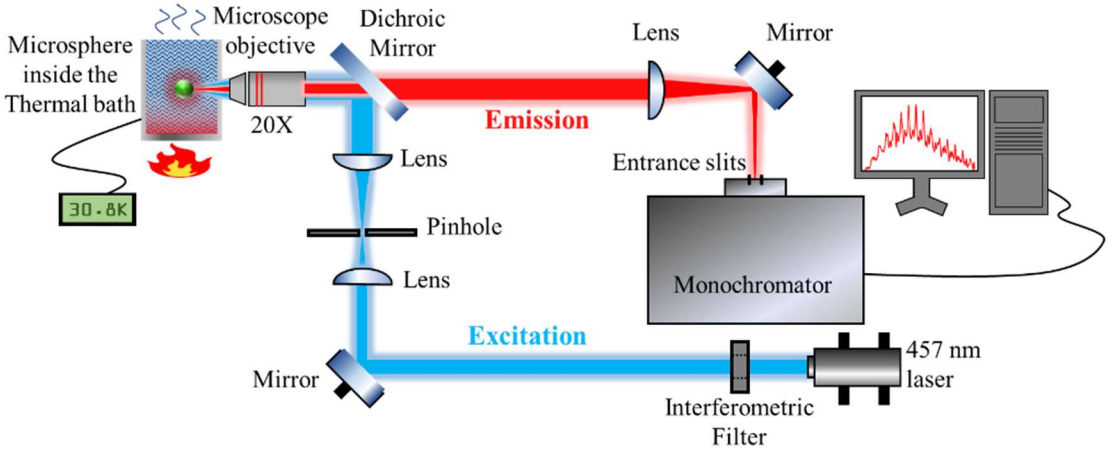

Fig. 1. Scheme of the setup used for the excitation, heating and detection of the WGM from the microspheres.

For the temperature calibration of the sensor, measurements for LIR experiments were performed placing a bulk sample inside a tubular furnace and using a simplified version to the one described above. The furnace was heated from RT to 482 K and a thermocouple was placed to detect the exact temperature of the sample (Fig. 2). For the WGM calibration as function of the temperature, the microspheres were placed inside a controlled thermal bath, so that the temperature of the microspheres could be regulated, and heated from RT up to 330 K (Fig. 1). It was not possible to heat up to 482 K due to the technical limitations of the thermal bath.

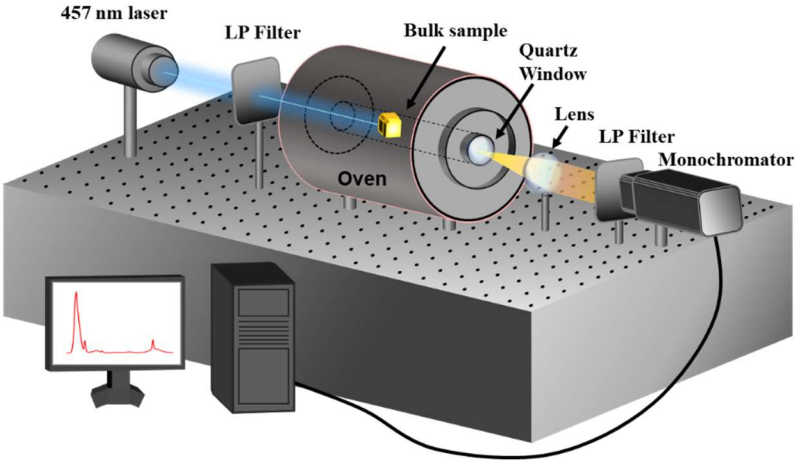

Fig. 2. Scheme of the setup used for the excitation, heating and detection of the bulk sample for the LIR measurements.

In order to determine the uncertainty of the LIR and WGM results as a function of temperature, 100 measurements were carried out in the same conditions at RT. The same band ratios used for the LIR were analyzed for these 100 measurements and a statistical study led to a standard deviation of 9.6×10^{-4} ratio. In the case of WGM, the spectral position of 6 WGM were analyzed for the 100 measurements obtaining a standard deviation of 7.3 pm. The error bars corresponding to these parameters were taken as the double of those standard deviations.

2. Results and discussion

The absorption spectrum of the $0.1Pr^{3+}$-$1.2Yb^{3+}$ co-doped phosphate glass was presented in Fig. 3. The bands assigned in the VIS at 443, 466 and 478 nm and a weak one at 587 nm are related to the transitions of Pr^{3+}: $^3H_4 \rightarrow {}^3P_0, {}^3P_1, {}^3P_2$ and $^1D_2$ [17], respectively. In addition, it was noticed the presence of peaks in NIR at 1441, 1538, 1938 and 2273nm corresponding to the transitions from $^3H_4$ to $^3F_4$, $^3F_3$, $^3F_2$and $^3H_6$, respectively [18]. Furthermore, a strong absorption band centered at 975nm in the NIR was observed, it is due to the $^2F_{7/2} \rightarrow {}^2F_{5/2}$electronic transition of Yb^{3+} ions [19].

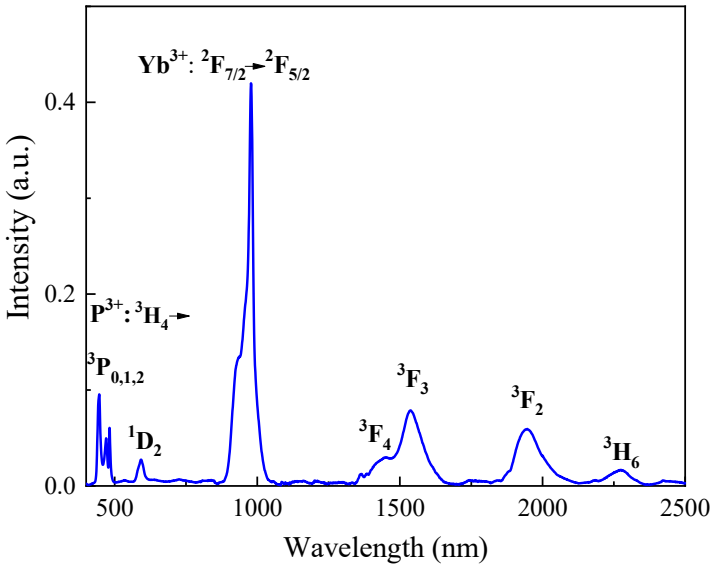

Fig. 3. Absorption spectrum of $0.1Pr^{3+}$-$0.5Yb^{3+}$ co-doped phosphate glass.

The emission spectra of the sample in the Vis-NIR spectral range (λex=457 nm) is shown in Fig. 4a. It can be noticed the presence of an intense peak at 605 nm corresponding to the Pr^{3+} transition $^1D_2 \rightarrow {}^3H_4$, and weak bands centered at 523 nm ($^3P_1 \rightarrow {}^3H_5$), 640 nm ($^3P_0 \rightarrow {}^3F_2$), 696 nm ($^3P_0 \rightarrow {}^3F_3$), 722 nm ($^3P_0 \rightarrow {}^3F_4$), 808-860 nm ($^1D_2 \rightarrow {}^3H_{6,5}$). In addition, a stronger peak located at 975 nm and a weaker peak at 1002 nm can be seen. These peaks correspond to the $^2F_{5/2} \rightarrow {}^2F_{7/2}$ transition of Yb^{3+} due to the DC process from Pr^{3+} to Yb^{3+} ions [20], schematized in Fig. 4b.

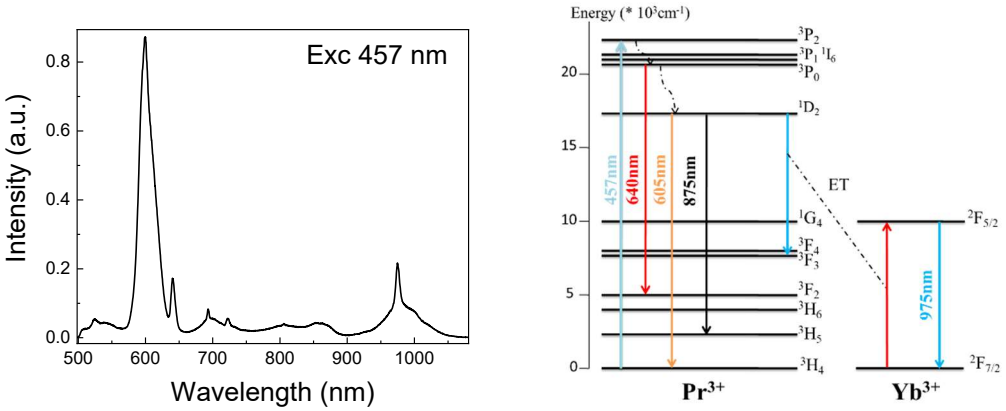

Fig. 4. **(a)** Normalized emission spectra of $0.1Pr^{3+}$-$0.5Yb^{3+}$ co-doped phosphate bulk glass excited with a 457 nm laser. **(b)** Energy level diagram showing the main emission transitions and energy transfer mechanism between Pr^{3+} and Yb^{3+} ions.

Furthermore, when the confocal setup was used and the detection was set to an edge of the microsphere, to selectively detect the light trapped inside the microsphere in the form of WGM, the spectrum drastically changed. A series of narrow peak, corresponding to the WGM phenomenon, appeared superimposed to the previous emission spectrum as it can be seen in Fig. 5. These sharp peaks correspond to the possible modes of the light that is trapped by total internal reflection in the spherical geometry of the microspheres.

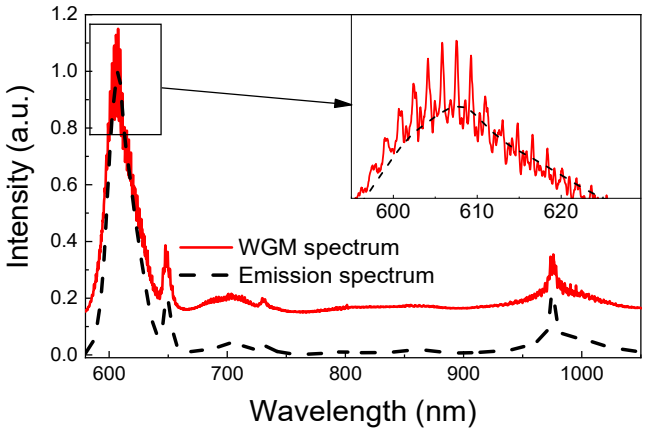

Fig. 5. Regular and WGM spectra of the $0.1Pr^{3+}$-$0.5Yb^{3+}$ co-doped phosphate glass microsphere excited with a 457 nm laser. Inset shows an amplification of the maximum of the emission peak at 605 nm.

For the temperature calibration, the sample was placed inside of a furnace an excited with a 457 nm laser and the emission was recorded from RT up to 482 K. When increasing the temperature, the influence of the temperature can be detected in the change of the band intensities as it can be seen in Fig. 6a. For calibration purposes, the ratio of the highest and lowest temperature spectra recorded was obtained and maximum and minimum values at 925 and 875 nm were observed, respectively (Fig. 6b). The intensity ratio from these wavelengths was used from RT up to 482 K to calibrate the sensor and was fitted to a cubic polynomial, as it can be seen in Fig. 7a.

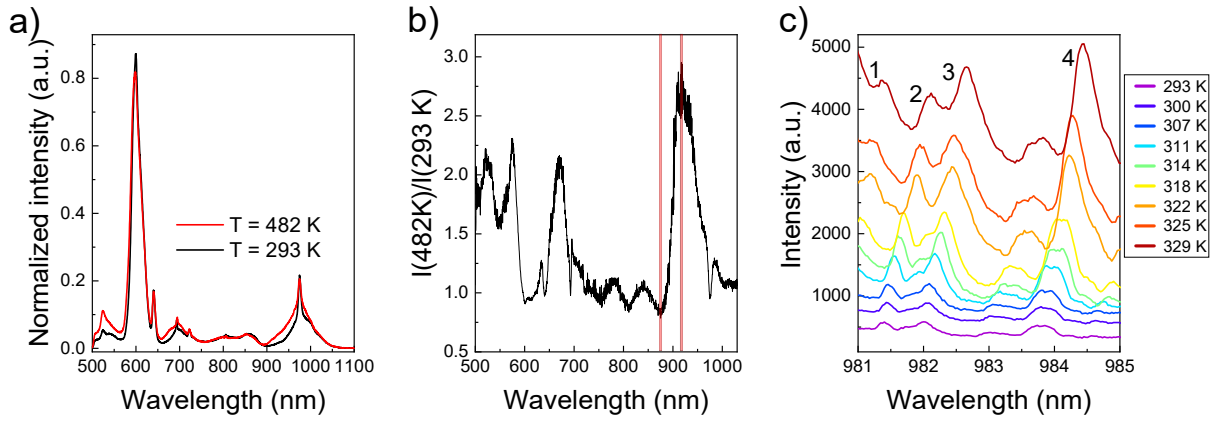

Fig. 6. **(a)** Spectra for the $0.1Pr^{3+}$-$0.5Yb^{3+}$ co-doped phosphate glass sample at 291 and 482 K, **(b)** Ratio from the previously mentioned spectra where the wavelengths used for the calibration with temperature has been marked with vertical lines and **(c)** red-shift of four of the six WGM recorded as a function of temperature (numbers indicate some of the modes used in the calculation of the red shift).

In the case of the WGM, a microsphere was placed inside a controlled thermal bath. As temperature increased, aside from the changes in the band ratio, a red-shift was observed for all the modes (Fig. 6c). The dependence of the resonant modes of the WGM can be described in terms of the geometrical optic ray approximation by [21]:

$$\lambda_m = \frac{2\pi}{m} \cdot n_{eff} R \tag{1}$$

where m is the mode number, λ_m are the resonant wavelengths, n_{eff} is the effective refractive index and R the radius of the microsphere. Following this equation, an increase in the temperature of the microsphere should lead to a red-shift of the resonant wavelengths given by:

$$\frac{d\lambda_m}{dT} = \frac{2\pi}{m} \cdot \left(n_{eff} \frac{dR}{dT} + R \frac{dn_{eff}}{dT} \right) = \lambda_m (\alpha + \beta) \tag{2}$$

where T is the temperature and α and β are the thermal expansion and thermo-optic coefficients, respectively.

Two things should be noticed from Eq. 2. First, due to the appearance of resonant modes throughout all Pr^{3+} and Yb^{3+} bands, by using WGM for temperature calibration, it is possible to measure in a wide range of wavelengths from 500 to more than 1000 nm. This is of special interest because these emissions cover the first optical window in biological experiments (I-BW), which

range from 800 to 900 nm. Second, the observed red-shift is only related to the thermal expansion and thermo-optic coefficients of the microsphere and the selected wavelength. Following this reasoning, this shift was recorded for six different modes (centered at 976.9, 978.0, 978.8, 981.4, 982.0 and 083.8 at RT) and its mean spectral shift is presented in Fig. 7b from RT up to 330 K with an average displacement of 0.024 nm/K. The selected modes were close in range, from 975 to 985 nm approximately, to minimize the effect of the wavelength described in Eq. 2.

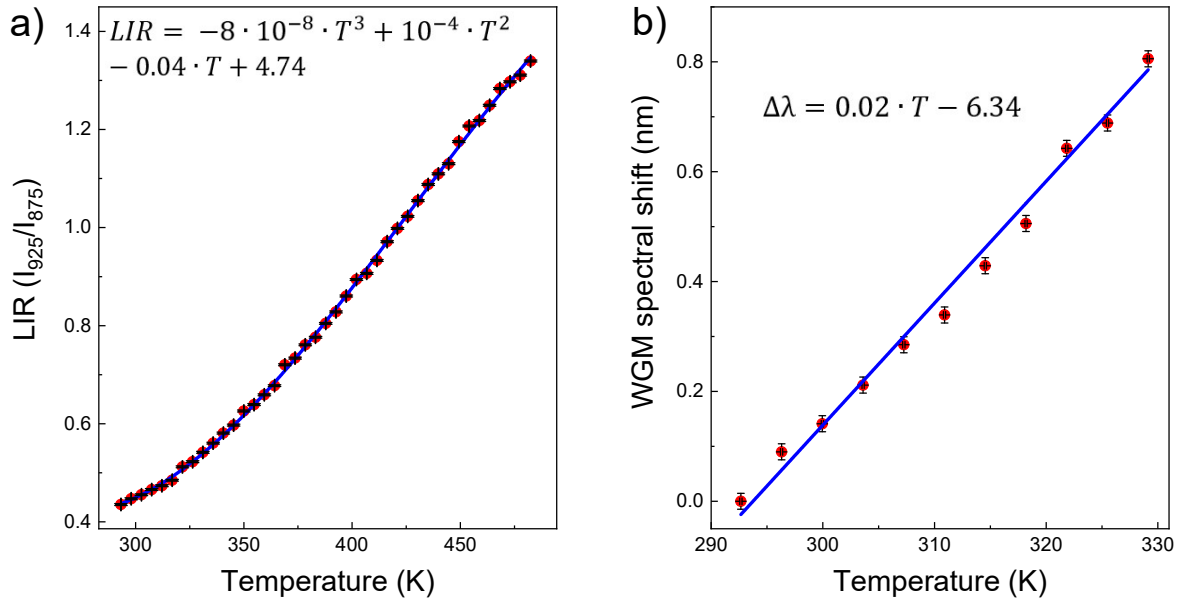

Fig. 7. (a) LIR of the 925/875 Pr^{3+}-Yb^{3+} bands and **(b)** WGM mean spectral shift for six different modes of the co-doped phosphate glass as a function of temperature.

In order to obtain the temperature uncertainty of Pr^{3+}-Yb^{3+} co-doped phosphate microspheres as temperature sensors, 100 measurements at ambient conditions were performed exciting a microsphere with a 457 nm laser to obtain both, Pr^{3+}-Yb^{3+} regular and WGM emission. From these 100 measurements, LIR as well as the spectral position of WGM (using the same mean 6 modes described in the previous paragraph) were obtained and the result for the different outcomes (number of measurements vs LIR value or WGM spectral position obtained in each measurement) are shown in Fig. 8. The uncertainty was taken as the standard deviation obtained from the statistical distribution of the 100 LIR results and WGM spectral positions (Fig. 8a and c). The equivalent uncertainty values for temperature were estimated using the fitting equations from Fig. 7a and b. An uncertainty of 0.7 K was obtained for the LIR (Fig. 8b), whereas for the WGM, the temperature uncertainty was of 0.4 K (Fig. 8d), showing an improvement of 0.3 K over the LIR

technique. Similar values, ranging from 0.5 to over 1 K are usually found in the literature for optical temperature sensors based on RE [22–26].

The error bars used for the LIR and WGM shift results presented in Fig. 7, correspond to the double of the uncertainty values obtained as it was described in the previous section. For the temperature axis, the standard error for a type-K thermocouple was used.

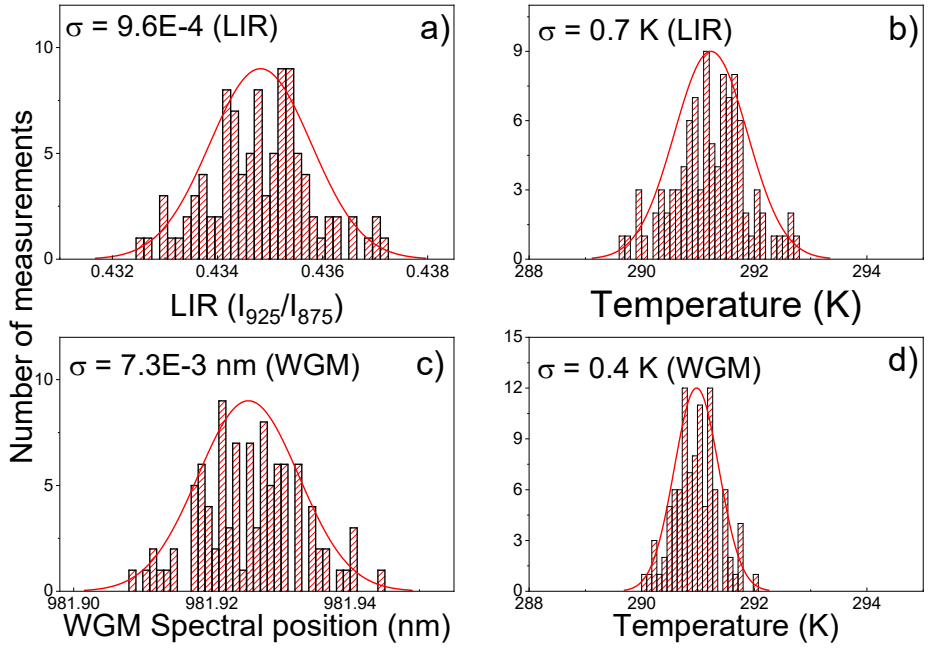

Fig. 8. Histograms of 100 measurements of $0.1Pr^{3+}$-$0.5Yb^{3+}$ co-doped phosphate microspheres at RT for LIR **(a)** and WGM spectral positions **(c)** with their respective standard deviations and equivalent temperatures **(b)** and **(d)**.

3. Conclusions

$0.1Pr^{3+}$-$0.5Yb^{3+}$ co-doped phosphate glass was synthesized and microsphere of diameters ranging from 30 μm to 100 μm were fabricated from the precursor glass. Under 457 nm laser excitation, the microspheres showed the typical emission of Pr^{3+} ions as well as emission due to a DC process from Pr^{3+} to Yb^{3+} ions. When heated, it was possible to calibrate the microspheres as a temperature sensor using the LIR technique as well as the spectral shift of WGM. The ratio of the 925 and 875 nm Pr^{3+} bands were recorded from RT up to 482 K, whereas WGM shift was recorded for six different modes from RT up to 330 K. The results were fitted and, following this fitting equation and a statistical analysis from 100 measurements at RT, the temperature uncertainty of the sensor was obtained for both techniques. Uncertainties of 0.7 K and 0.4 K were obtained for the LIR and WGM results, respectively. These low uncertainty values and the possibility of using two methods for temperature calibration (with emissions at different wavelengths that are within the I-BW)

make microspheres from $0.1Pr^{3+}$-$0.5Yb^{3+}$ co-doped phosphate glass a promising candidate in the world of contactless optical temperature sensors.

Acknowledgments

This work is supported by the ministry of higher education and scientific research of Tunisia, Ministerio de Ciencia e Innovación of Spain (MICIIN) under the National Program of Sciences and Technological Materials (PID2019-106383GB-C44 and PID2019- 107335RA-I00), Gobierno de Canarias (ProID2020010067) and EU-FEDER funds.

References

[1] L.D. Carlos, F. Palacio, Thermometry at the nanoscale: Techniques and selected applications, Royal Society of Chemistry, 2015.

[2] C. Gota, K. Okabe, T. Funatsu, Y. Harada, S. Uchiyama, Hydrophilic Fluorescent Nanogel Thermometer for Intracellular Thermometry, J. Am. Chem. Soc. 131 (2009) 2766–2767. doi:10.1021/ja807714j.

[3] O. Zohar, M. Ikeda, H. Shinagawa, H. Inoue, H. Nakamura, D. Elbaum, D.L. Alkon, T. Yoshioka, Thermal Imaging of Receptor-Activated Heat Production in Single Cells, Biophys. J. 74 (1998) 82–89. doi:10.1016/S0006-3495(98)77769-0.

[4] A. Martínez-González, D. Moreno-Hernández, J.A. Guerrero-Viramontes, J.C.I. Zamarripa-Ramírez, C. Carrillo-Delgado, Multiplane temperature measurement of fluid flows using a color focusing schlieren system, Opt. Laser Technol. 142 (2021) 107256. doi:10.1016/j.optlastec.2021.107256.

[5] V.K. Rai, Temperature sensors and optical sensors, Appl. Phys. B. 88 (2007) 297–303. doi:10.1007/s00340-007-2717-4.

[6] Y. Zhou, F. Qin, Y. Zheng, Z. Zhang, W. Cao, Fluorescence intensity ratio method for temperature sensing, Opt. Lett. 40 (2015) 4544. doi:10.1364/OL.40.004544.

[7] S. Zhou, X. Li, X. Wei, C. Duan, M. Yin, A new mechanism for temperature sensing based on the thermal population of 7 F 2 state in Eu 3+, Sensors Actuators B Chem. 231 (2016) 641–645. doi:10.1016/j.snb.2016.03.082.

[8] C. Jin, J. Zhang, Upconversion luminescence of Ca2Gd8(SiO4)6O2:Yb3+-Tm3+-Tb3+/Eu3+ phosphors for optical temperature sensing, Opt. Laser Technol. 115 (2019) 487–492. doi:10.1016/j.optlastec.2019.02.058.

[9] M. Runowski, A. Bartkowiak, M. Majewska, I.R. Martín, S. Lis, Upconverting

lanthanide doped fluoride NaLuF4:Yb3+-Er3+-Ho3+ - optical sensor for multi-range fluorescence intensity ratio (FIR) thermometry in visible and NIR regions, J. Lumin. 201 (2018) 104–109. doi:10.1016/j.jlumin.2018.04.040.

[10] M.A. Hernández-Rodríguez, M.M. Afonso, J.A. Palenzuela, I.R. Martín, K. Soler-Carracedo, Carbon dots as temperature nanosensors in the physiological range, J. Lumin. 196 (2018) 313–315. doi:10.1016/j.jlumin.2017.12.062.

[11] C.D.S. Brites, A. Millán, L.D. Carlos, Lanthanides in Luminescent Thermometry, in: 2016: pp. 339–427. doi:10.1016/bs.hpcre.2016.03.005.

[12] T. Reynolds, N. Riesen, A. Meldrum, X. Fan, J.M.M. Hall, T.M. Monro, A. François, Fluorescent and lasing whispering gallery mode microresonators for sensing applications, Laser Photon. Rev. 11 (2017) 1600265. doi:10.1002/lpor.201600265.

[13] X. Jiang, A.J. Qavi, S.H. Huang, L. Yang, Whispering gallery microsensors: a review, ArXiv Prepr. ArXiv1805.00062. (2018).

[14] G.R. Elliott, D.W. Hewak, G.S. Murugan, J.S. Wilkinson, Chalcogenide glass microspheres; their production, characterization and potential, Opt. Express. 15 (2007) 17542. doi:10.1364/OE.15.017542.

[15] V. Lefèvre-Seguin, Whispering-gallery mode lasers with doped silica microspheres, Opt. Mater. (Amst). 11 (1999) 153–165. doi:10.1016/S0925-3467(98)00041-X.

[16] C.G.B. Garrett, W. Kaiser, W.L. Bond, Stimulated Emission into Optical Whispering Modes of Spheres, Phys. Rev. 124 (1961) 1807–1809. doi:10.1103/PhysRev.124.1807.

[17] Q.Y. Zhang, Z.M. Yang, G.F. Yang, Z.D. Deng, Z.H. Jiang, Enhanced blue-green-red up-conversion and 1.3-μm emission of Pr3+/Yb3+-codoped oxyhalide tellurite glasses with PbCl2 doping, J. Phys. Chem. Solids. 66 (2005) 1281–1286. doi:10.1016/j.jpcs.2005.05.003.

[18] R.S. Quimby, P.A. Tick, N.F. Borrelli, L.K. Cornelius, Quantum efficiency of Pr3+ doped transparent glass ceramics, J. Appl. Phys. 83 (1998) 1649–1653. doi:10.1063/1.366879.

[19] J. Zhou, Y. Teng, G. Lin, J. Qiu, Ultraviolet to near-infrared spectral modification in Ce3+ and Yb3+ codoped phosphate glasses, J. Non. Cryst. Solids. 357 (2011) 2336–2339. doi:10.1016/j.jnoncrysol.2010.11.080.

[20] Y. Huang, L. Luo, J. Wang, Q. Zuo, Y. Yao, W. Li, The down-conversion and up-conversion photoluminescence properties of Na 0.5 Bi 0.5 TiO 3 :Yb 3+ /Pr 3+ ceramics, J. Appl. Phys. 118 (2015) 044101. doi:10.1063/1.4927278.

[21] K. Soler-Carracedo, A. Ruiz, I.R. Martín, F. Lahoz, Luminescence whispering gallery

modes in Ho3+ doped microresonator glasses for temperature sensing, J. Alloys Compd. 777 (2019) 198–203. doi:10.1016/j.jallcom.2018.10.297.

[22] K. Soler-Carracedo, I.R. Martín, F. Lahoz, H.C. Vasconcelos, A.D. Lozano-Gorrín, L.L. Martín, F. Paz-Buclatin, Er3+/Ho3+ codoped nanogarnet as an optical FIR based thermometer for a wide range of high and low temperatures, J. Alloys Compd. 847 (2020) 156541. doi:10.1016/j.jallcom.2020.156541.

[23] C.D.S. Brites, K. Fiaczyk, J.F.C.B. Ramalho, M. Sójka, L.D. Carlos, E. Zych, Widening the Temperature Range of Luminescent Thermometers through the Intra- and Interconfigurational Transitions of Pr 3+, Adv. Opt. Mater. 6 (2018) 1701318. doi:10.1002/adom.201701318.

[24] F. Paz-Buclatin, S. Ríos, I.R. Martín, L.L. Martin, Fluorescence intensity ratio and whispering gallery mode techniques in optical temperature sensors: comparative study, Opt. Mater. Express. 9 (2019) 4126. doi:10.1364/OME.9.004126.

[25] H. Song, Q. Han, X. Tang, X. Zhao, K. Ren, T. Liu, Nd3+/Yb3+ codoped SrWO4 for highly sensitive optical thermometry based on the near infrared emission, Opt. Mater. (Amst). 84 (2018) 263–267. doi:10.1016/j.optmat.2018.06.054.

[26] R. Lei, D. Deng, X. Liu, F. Huang, H. Wang, S. Zhao, S. Xu, Influence of excitation power and doping concentration on the upconversion emission and optical temperature sensing behavior of Er 3+ : BaGd 2 (MoO 4) 4 phosphors, Opt. Mater. Express. 8 (2018) 3023. doi:10.1364/OME.8.003023.